Power-Law Shot Noise

STEVEN B. LOWEN, STUDENT MEMBER, IEEE, AND MALVIN C. TEICH, FELLOW, IEEE

Abstract —**The behavior of power-law shot noise, for which the associated impulse response functions assume a decaying power-law form, is explored. Expressions are obtained for the moments, moment generating functions, amplitude probability density functions, autocorrelation functions, and power spectral densities for a variety of parameters of the process. For certain parameters the power spectral density exhibits $1/f$-type behavior over a substantial range of frequencies, so that the process serves as a source of $1/f^{\alpha}$ shot noise for α in the range $0<\alpha<2$. For other parameters the amplitude probability density function is a Lévy-stable random variable with dimension less than unity. This process then behaves as a fractal shot noise that does *not* converge to a Gaussian amplitude distribution as the driving rate increases without limit. Fractal shot noise is a stationary continuous-time process that is fundamentally different from fractional Brownian motion. We consider several physical processes that are well described by power-law shot noise in certain domains: $1/f$ shot noise, Cherenkov radiation from a random stream of charged particles, diffusion of randomly injected concentration packets, the electric field at the growing edge of a quantum wire, and the mass distribution of solid-particle aggregates.**

Index Terms —**fractal process, Lévy-stable process, $1/f$ noise, power-law shot noise.**

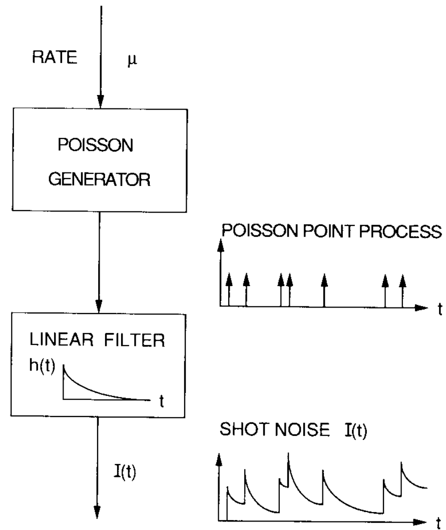

Fig. 1. Linearly filtered Poisson point process gives rise to shot noise. Rate of Poisson point process is μ, $h(t)$ represents impulse response function of linear filter, and $I(t)$ is shot-noise amplitude. Power-law shot noise results when $h(t)$ decays in power-law fashion.

I. Introduction and Summary of Results

In 1918 SCHOTTKY defined and extensively studied the shot-noise process and named it the shot effect [1]. In fact, certain aspects of this process had been studied since the beginning of the century; Campbell obtained values for the mean and variance of the process in 1909 [2], [3]. As schematically indicated in Fig. 1, shot noise results from the excitation of a memoryless, linear filter by a train of impulses derived from a homogeneous Poisson point process [4]–[7]. The former is characterized by its impulse response function $h(t)$, while the latter is characterized by its constant rate of production of events, μ. The shot effect is particularly visible in electrical devices at low currents, or indeed in any system where events occur with an average spacing greater than the characteristic time duration of each event. Under certain weak conditions, the central limit theorem shows that the amplitude distribution of shot noise approaches a Gaussian distribution as the rate of the driving Poisson process increases [4], [8]. Generally, if the rate μ is substantially greater than the reciprocal of the characteristic time duration of the impulse response function $1/\tau_p$, then the amplitude distribution will closely approximate a Gaussian form. The characteristic time τ_p is often defined as the square of the integral of the impulse response function divided by the integral of its square. Most common impulse response functions, such as triangles, rectangles, and decaying exponentials are well behaved, having a finite, nonzero characteristic time. Shot noises constructed from these impulse response functions will indeed approach a Gaussian distribution as the driving rate μ increases.

When the impulse response function is a decaying power law, however, its characteristic time can become arbitrarily large or small. Power-law shot noise can therefore violate the conditions of the central limit theorem, and yield an amplitude distribution that does not approach the Gaussian distribution for any value of the Poisson driving rate. Many physical situations exist in which power-law shot noise arises. A representative power-law impulse response function is shown in Fig. 2. For this particular illustration the onset time A of the impulse response function is unity, the termination time

Manuscript received November 16, 1989; revised March 19, 1990. This work was supported by the National Science Foundation through the Columbia Center for Telecommunications Research and by the Joint Services Electronics Program through the Columbia Radiation Laboratory.

The authors are with the Columbia Radiation Laboratory and the Center for Telecommunications Research, Department of Electrical Engineering, Columbia University, New York, NY 10027.

IEEE Log Number 9036817.

0018-9448/90/1100-1302$01.00

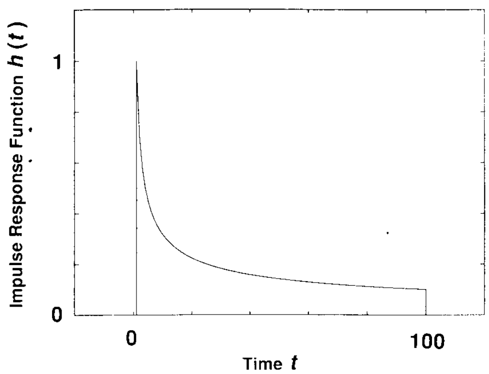

Fig. 2. Linear plot of particular power-law impulse response function $h(t)$ vs. time t ($\beta = 1/2$, $A = 1$, $B = 100$, $K_0 = 1$).

$B = 100$, the power-law exponent β is $1/2$, and the amplitude K_0 is unity.

We proceed to derive the statistical properties of power-law shot noise, including its moments, moment generating functions, amplitude probability density functions, autocorrelation functions, and power spectral densities. Power-law shot noise in the regime $0 < \beta < 1$ [9] differs markedly from power-law shot noise for $\beta > 1$ [10], and thus two types of novel behavior emerge.

For linear-filter parameters in the range $0 < \beta < 1$ and $B < \infty$, the resulting power spectral density varies as $1/f^{\alpha}$ over a substantial range of frequencies f. The exponent $\alpha = 2(1 - \beta)$ can assume values between 0 and 2 [11], [12], so that the process behaves as a source of $1/f$-type shot noise. For $\alpha = 1$, the power spectral density varies precisely as $1/f$.

For linear-filter parameters in the range $\beta > 1$ and $A = 0$, the resulting shot-noise amplitude distribution assumes the form of a Lévy-stable random variable [8], [13], [14] of extreme asymmetry and dimension $D < 1$. In this case, the amplitude distribution does not converge to a Gaussian form, and in particular the associated mean and variance are infinite. This fractal shot-noise process should be contrasted with fractional Brownian motion (FBM), developed by Mandelbrot and Van Ness [15], [16]. Fractional Brownian motion usually has a Gaussian amplitude distribution, but the times between zero crossings have a Lévy-stable time-interval distribution. Our Lévy-stable process, in contrast, has a Lévy-stable amplitude distribution and no zero crossings. In addition, the fractal nature of our Lévy-stable shot-noise process differs from that of FBM, which is self-affine and nonstationary; our Lévy-stable process is strict-sense stationary.

In Fig. 3, we present a summary of the forms assumed by the amplitude probability density function and power spectral density of power-law shot noise for various ranges of its parameters. Novel results are indicated by regions of the figure delineated by thick boxes. Depending on the values of β [or equivalently, the values of $\alpha \equiv 2(1 - \beta)$ for $0 < \beta < 1$ and $D \equiv 1/\beta$ for $\beta > 1$], A, and B, there are six possibilities for the amplitude probability distribution of the shot-noise process I.

1) $\Pr\{I = \infty\} = 1$: The amplitude I is infinite with probability one, and therefore the mean, autocorrelation function, and variance are also infinite.
2) $I =$ Lévy-stable: The amplitude I is a one-sided Lévy-stable random variable with dimension $D \equiv 1/\beta$ for all values of μ, and therefore the mean, autocorrelation function, and variance are infinite.
3) $I \to$ Lévy-stable: The amplitude I approaches a one-sided Lévy-stable random variable with dimension $D \equiv 1/\beta$ as $\mu \to \infty$. The mean, autocorrelation function, and variance are infinite for all values of μ.
4) I.M./I.V.: The mean, autocorrelation function, and variance of the process are infinite, but $\Pr\{I = \infty\} < 1$, and the probability density function is not Lévy-stable.
5) F.M./I.V.: The mean and the autocorrelation function (for all $\tau > 0$) of the process are finite for all finite values of μ, but the variance is infinite.
6) $I \to$ Gaussian: The mean, autocorrelation function, and variance are all finite. Therefore the amplitude approaches a Gaussian random variable as $\mu \to \infty$.

Depending on the values of β [or equivalently, the values of $\alpha \equiv 2(1 - \beta)$ for $0 < \beta < 1$ and $D \equiv 1/\beta$ for $\beta > 1$], A, and B, there are five possibilities for the power spectral density of the shot-noise process I.

1) no $H(f)$: The impulse response function does not have a well-defined Fourier transform. The power spectral density, $S_I(f)$, cannot exist in this case either.
2) $|H(f)|^2$ not $1/f^{\alpha}$: The impulse response function has a well-defined Fourier transform, but the square of its magnitude does not vary as an inverse power of the frequency. The power spectral density does not exist.
3) $|H(f)|^2 \sim 1/f^{\alpha}$: The impulse response function has a well-defined Fourier transform, and the square of its magnitude varies as $1/f^{\alpha}$ over a range of frequencies f. If $A > 0$, then $1/f$-type behavior is exhibited only for $f \ll 1/A$; if $B < \infty$, then only for $f \gg 1/B$. The power spectral density does not exist.
4) $S_I(f)$ not $1/f^{\alpha}$: The shot-noise process $I(t)$ has a well-defined power spectral density, but it does not vary as an inverse power of the frequency.
5) $S_I(f) \sim 1/f^{\alpha}$: The shot-noise process $I(t)$ has a well-defined power spectral density, which varies as $1/f^{\alpha}$ over a range of frequencies f. If $A > 0$, then $1/f$-type behavior is exhibited only for $f \ll 1/A$; if $B < \infty$, then only for $f \gg 1/B$.

We refer to the process at hand as power-law shot noise because, aside from the impulse response function itself, three of its properties can be characterized by power-law functions: the amplitude probability density, the autocorrelation function, and the power spectral density. Furthermore, the autocorrelation function and the impulse response function share the same exponent. Power-law dependencies indicate the presence of all time

	$A>0$ & $B=\infty$	$A=0$ & $B=\infty$	$A=0$ & $B<\infty$	$A>0$ & $B<\infty$
$0<\beta<1/2$ $(2>\alpha>1)$	$\Pr\{I=\infty\}=1$ $\lvert H(f)\rvert^2 \sim 1/f^\alpha$	$\Pr\{I=\infty\}=1$ $\lvert H(f)\rvert^2 \sim 1/f^\alpha$	$I \to$ Gaussian $S_I(f)\sim 1/f^\alpha$	$I \to$ Gaussian $S_I(f)\sim 1/f^\alpha$
$1/2\le\beta<1$ $(1\ge\alpha>0)$	$\Pr\{I=\infty\}=1$ $\lvert H(f)\rvert^2 \sim 1/f^\alpha$	$\Pr\{I=\infty\}=1$ $\lvert H(f)\rvert^2 \sim 1/f^\alpha$	F.M./I.V. $S_I(f)\sim 1/f^\alpha$	$I \to$ Gaussian $S_I(f)\sim 1/f^\alpha$
$\beta=1$	$\Pr\{I=\infty\}=1$ $\lvert H(f)\rvert^2$ not $1/f^\alpha$	$\Pr\{I=\infty\}=1$ no $H(f)$	I.M./I.V. no $H(f)$	$I \to$ Gaussian $S_I(f)$ not $1/f^\alpha$
$\beta>1$ $(0<D<1)$	$I \to$ Gaussian $S_I(f)$ not $1/f^\alpha$	$I=$ Lévy-stable no $H(f)$	$I \to$ Lévy-stable no $H(f)$	$I \to$ Gaussian $S_I(f)$ not $1/f^\alpha$

Fig. 3. Summary of forms assumed by the amplitude probability distribution function and power spectral density of power-law shot noise for various ranges of its parameters f, A, B (see text). Novel results are delineated by thick boxes.

scales, and therefore fractal behavior.

In the final section of the paper, we consider several applications of power-law shot noise, illustrating its widespread applicability. Power-law behavior is common in nature: electromagnetic forces vary as the inverse square of the distance, diffusion processes often exhibit power-law tails, and $1/f$ noise is power law by definition. Our applications are chosen from among these naturally occurring power-law dependencies.

II. Shot Noise

A. General Shot Noise

Shot noise may be expressed as an infinite sum of impulse response functions, which may be either stochastic or deterministic (see Fig. 1). If deterministic, then the definition of the shot noise amplitude $I(t)$ is

$$I(t) \equiv \sum_{j=-\infty}^{\infty} h(t-t_j). \tag{1}$$

The times t_j are random events from a homogeneous Poisson point process of rate μ, and the impulse response function $h(\cdot)$ is fixed and deterministic (the linear system is time-invariant). If the impulse response functions are stochastic, then the definition of the shot noise becomes

$$I(t) \equiv \sum_{j=-\infty}^{\infty} h(K_j, t-t_j). \tag{2}$$

Here the times t_j are as before, and $\{K_j\}$ is a random sequence over which the impulse response functions $h(K,t)$ are indexed. The elements of the random sequence $\{K_j\}$ are taken to be identically distributed, and independent of each other and of the Poisson process. The impulse response function $h(\cdot,\cdot)$ is itself deterministic.

The properties of shot noise become more difficult to obtain if the component impulse response functions are stochastic rather than deterministic. However, it is possible to find an equivalent impulse response function that is indeed deterministic. This equivalent function will not necessarily lead to correct results when it is used in calculating second- or higher-order statistics, such as the autocorrelation function or the power spectral density, but for first-order properties of the shot-noise process, this function is truly equivalent to the ensemble of stochastic impulse response functions. Gilbert and Pollak [17] have shown that such an ensemble of stochastic impulse response functions $\{h(K,t)\}$ has an equivalent deterministic impulse response function satisfying

$$\langle \mathscr{L}\{t: h(K,t)>x\}\rangle = \mathscr{L}\{t: h(t)>x\}, \tag{3}$$

for all x, where $\mathscr{L}$ denotes the Lebesgue set measure, and $\langle\cdot\rangle$ represents expectation taken over the distribution of K. In particular, any impulse response function of the form $h(K,t)=h(t/K)$ is equivalent to an impulse response function of the form $h(t/\langle|K|\rangle)$. An equivalent impulse response function may always be found for any ensemble of stochastic impulse response functions, but in general the equivalent impulse response function will not resemble the component impulse response functions of the ensemble. Finally, we reiterate that equivalent impulse response functions are only equivalent for the first-order statistics of the shot-noise process; equivalent deterministic impulse response functions may not be used for higher-order statistics.

All properties are valid after the shot-noise process has reached steady-state, when the time t is finite. For completeness we note that for the impulse response functions considered in Section IV-C, the resulting shot-noise process never reaches steady-state. For these degenerate processes, the results derived in this paper do not apply for any time t.

B. Power-Law Shot Noise

The general form of the power-law impulse response function that we choose is

$$h(K,t) \equiv \begin{cases} Kt^{-\beta}, & A \le t < B; \\ 0, & \text{otherwise}, \end{cases} \tag{4}$$

an example of which is shown in Fig. 2. The parameters A, B, and β, are deterministic and fixed. In general, the range of the function may extend down to $A = 0$ or up to $B = \infty$, and β may range between 0 and ∞ exclusive. The amplitude parameter may be either random (denoted by K) or deterministic (denoted by K_0). All parameters are assumed to be nonnegative. Thus power-law impulse response functions as previously defined are either deterministic, in which case all component impulse response functions are identical, or have random amplitudes, in which case the component impulse response functions have the same shape and duration, differing only in their amplitudes K.

Although we choose to consider power-law impulse response functions such that those from the same shot-noise process can differ only in their amplitudes, our results may be extended in some cases to generalized power-law impulse response functions. As shown in Section II-A, an equivalent, deterministic impulse response function may be found for any ensemble of stochastic impulse response functions of the form $h(K,t)$ [17]. If the resulting equivalent impulse response function is of the form shown in (4), then the equivalent impulse response function may be substituted for calculations of first-order amplitude statistics of the original, stochastic shot-noise process. Substituting (4) into (3) we show that any impulse response function satisfying

$$\langle \mathscr{L}\{t: h(K,t) > x\} \rangle = \begin{cases} \infty, & x < 0; \\ B - A, & 0 \le x \le K_0 B^{-\beta}; \\ (x/K_0)^{-1/\beta} - A, & K_0 B^{-\beta} < x < K_0 A^{-\beta}; \\ 0, & x \ge K_0 A^{-\beta}; \end{cases} \tag{5}$$

for some β, A, B, and K_0, is equivalent to the deterministic impulse response function

$$h(t) = \begin{cases} K_0 t^{-\beta}, & A \le t < B; \\ 0, & \text{otherwise}. \end{cases} \tag{6}$$

Thus first-order amplitude results derived for a shot-noise process constructed from the deterministic impulse response function in (6) will also apply to a process constructed from the generalized stochastic form in (5). In general, it is difficult to find a nontrivial ensemble of impulse response functions for which the equivalent impulse response function is of the form in (6). However, returning to (4) and considering the particular case $A = 0$ and $B = \infty$ we find

$$\begin{aligned} &\langle \mathscr{L}\{t: h(K,t) > x\} \rangle \\ &\quad = \langle \mathscr{L}\{t: Kt^{-\beta} > x\} \rangle = \langle \mathscr{L}\{t: t < K^{1/\beta} x^{-1/\beta}\} \rangle \\ &\quad = \langle K^{1/\beta} \rangle x^{-1/\beta}, \end{aligned} \tag{7}$$

for all positive amplitudes x. For the deterministic power-law impulse response function

$$\begin{aligned} &\mathscr{L}\{t: h(t) > x\} \\ &\quad = \mathscr{L}\{t: K_0 t^{-\beta} > x\} = \mathscr{L}\{t: t < K_0^{1/\beta} x^{-1/\beta}\} \\ &\quad = K_0^{1/\beta} x^{-1/\beta}, \end{aligned} \tag{8}$$

again for all positive amplitudes x. Thus the stochastic ensemble of impulse response functions in (7) is equivalent to the deterministic impulse response function in (8) for all first-order amplitude statistics with

$$\langle K^{1/\beta} \rangle = K_0^{1/\beta}, \tag{9}$$

so that

$$K_0 \equiv \langle K^{1/\beta} \rangle^{\beta}. \tag{10}$$

For $A > 0$ or $B < \infty$, (7) and (8) no longer agree for all x, and therefore the equivalent impulse response function does not have the form of (8). In that case, the stochastic amplitudes must be accounted for explicitly.

III. Moments and Cumulants

We consider the case of power-law shot noise when K is stochastic. The nth cumulant (semiinvariant) C_n of $I(t)$ is given by [18]

$$\begin{aligned} C_n &\equiv (-1)^n \frac{d^n}{ds^n} \ln Q_I(s) \bigg|_{s=0} = \mu \left\langle \int_{-\infty}^{\infty} h^n(t)\, dt \right\rangle \\ &= \mu \langle K^n \rangle \int_A^B t^{-n\beta}\, dt, \end{aligned} \tag{11}$$

so that

$$C_n = \mu \langle K^n \rangle \times \begin{cases} \dfrac{A^{1-n\beta} - B^{1-n\beta}}{n\beta - 1}, & \beta \ne 1/n; \\ \ln(B/A), & \beta = 1/n; \end{cases} \tag{12}$$

where $Q_I(s)$ is the first-order moment generating function of the shot-noise process I. The nth cumulant will be infinite if $\langle K^n \rangle$ is infinite, if $A = 0$ and $\beta \ge 1/n$, or if $B = \infty$ and $\beta \le 1/n$. All moments of I may be given in terms of the cumulants. The first three moments and the variance are

$$\begin{aligned} E[I] &= C_1 & E[I^2] &= C_2 + C_1^2 \\ E[I^3] &= C_3 + 3C_1C_2 + C_1^3 & \text{var}(I) &= C_2, \end{aligned} \tag{13}$$

where $E[\cdot]$ denotes expectation taken over the distribution of I.

IV. Moment Generating Functions

A. Deterministic K_0

We first consider the case for deterministic and fixed K_0; therefore all impulse response functions are identical. The first-order moment generating function $Q_I(s)$ of the shot-noise process I is given by [4], [7], [19], [20]

$$Q_I(s) \equiv E[e^{-sI}] = \exp\left(-\mu \int_{-\infty}^{\infty} \{1 - \exp[-sh(t)]\}\, dt\right). \tag{14}$$

For a decaying power-law impulse response function

$$Q_I(s) = \exp\left\{-\mu \int_A^B [1 - \exp(-sK_0 t^{-\beta})]\, dt\right\} \tag{15}$$

$$= \exp\left\{-\frac{\mu(sK_0)^{1/\beta}}{\beta} \int_{sK_0 B^{-\beta}}^{sK_0 A^{-\beta}} \frac{1 - e^{-u}}{u^{1+1/\beta}}\, du\right\} \tag{16}$$

$$= \exp\left\{-\mu(B - A) - \frac{\mu(sK_0)^{1/\beta}}{\beta} \cdot \left[\Gamma(-1/\beta, sK_0 A^{-\beta}) - \Gamma(-1/\beta, sK_0 B^{-\beta})\right]\right\}, \tag{17}$$

where $\Gamma(\cdot,\cdot)$ is the incomplete gamma function defined by

$$\Gamma(a, x) \equiv \int_x^{\infty} e^{-t} t^{a-1}\, dt. \tag{18}$$

Equivalently, after integrating (16) by parts,[1]

$$\begin{aligned} Q_I(s) = \exp\{&\mu A[1 - \exp(-sK_0 A^{-\beta})] \\ &- \mu B[1 - \exp(-sK_0 B^{-\beta})] \\ &+ \mu(sK_0)^{1/\beta}\Gamma(1 - 1/\beta, sK_0 A^{-\beta}) \\ &- \mu(sK_0)^{1/\beta}\Gamma(1 - 1/\beta, sK_0 B^{-\beta})\}. \end{aligned} \tag{19}$$

Equations (17) and (19) may be used for numerically computing $Q_I(s)$ for all values of μ, A, B, K_0, and $\beta > 0$.

B. Lévy-Stable Forms ($\beta > 1$)

For $\beta > 1$, if we let $A = 0$ and $B = \infty$, then a much simpler form for $Q_I(s)$ results. After evaluating limits using l'Hôpital's rule, we obtain

$$Q_I(s) = \exp\left[-\mu(sK_0)^{1/\beta}\Gamma(1 - 1/\beta)\right]. \tag{20}$$

Defining $D \equiv 1/\beta$ for $\beta > 1$, we have $0 < D < 1$. Furthermore, for $A = 0$ and $B = \infty$, we can consider stochastic K by using the equivalent deterministic impulse response function method of Gilbert and Pollak [17], which leads to

$$Q_I(s) = \exp\left[-\mu\langle K^D\rangle\Gamma(1 - D)s^D\right]. \tag{21}$$

Note that $K_0^D = \langle K^{1/\beta}\rangle = \langle K^D\rangle$. This moment generating function is of the form

$$Q(s) = \exp\left[-(cs)^D\right], \tag{22}$$

where c is a constant, so that for all μ the shot noise I is a Lévy-stable random variable [8], [13], [14], [21] with extreme asymmetry of dimension D: $0 < D < 1$. The Lévy-stable and Gaussian distributions share the property that two random variables taken from the same distribution and added together will result in a new random variable whose distribution differs from the original one only by a scaling constant. Thus, by definition, increasing μ, which is equivalent to adding two such processes together, will not change the Lévy-stable form of the resulting distribution. Therefore an infinite area impulse response function may be used to construct a shot-noise process which is nontrivial and non-Gaussian for all driving rates μ, even in the limits $\mu \to 0$ and $\mu \to \infty$. The conditions of the Gaussian central limit theorem are violated, and in particular all moments of the shot-noise process are infinite.

C. Other Infinite-Area Impulse Response Functions

However, for other infinite-area impulse response functions the resulting shot noise can have trivial amplitude properties. For $0 < \beta \le 1$ and $B = \infty$, the shot-noise process I will be infinite with probability one (see Appendix A). To show this, we derive the moment generating function $Q_I(s)$ for this case

$$Q_I(s) = \begin{cases} 1, & s = 0, \\ 0, & s \ne 0; \end{cases} \tag{23}$$

so that

$$\Pr\{I < x\} = 0, \qquad \text{for all } x < \infty. \tag{24}$$

This may be appreciated intuitively by examining the time evolution of the shot-noise process. Consider the system at time $t = -\infty$, when $I(t) = 0$, before any events from the driving Poisson process have occurred, and therefore before any of the component impulse response functions have begun. Since each impulse response function contains infinite area in its tail, the power-law shot-noise process $I(t)$ will tend to increase with time. In particular, $\Pr\{I(t) < x\}$ is a monotone decreasing function of t for any fixed amplitude x. Thus for $\beta \le 1$ and $B = \infty$, $I(t)$ is nonstationary, never reaching steady-state, and for finite times t will be infinite with probability one.

The difference between trivial and nontrivial amplitude properties appears to lie in the nature of the infinity in the impulse response function. For $\beta > 1$, the infinite area is contained in the infinitesimal neighborhood of $t = 0$, and therefore only manifests itself at the times $t = t_j$, corresponding to the events of the driving homogeneous Poisson process. The remainder of the time the process is finite. However, for $\beta \le 1$, the tail, which lasts for infinite time, contains infinite area. Since the tails of previous impulse response functions are always present, the process is always infinite. The case $\beta = 1$ is particularly unrewarding, since both the infinitesimal neighborhood of $t = 0$ and the tail contain infinite area.

D. Moment Generating Functions with Finite Moments

If the cumulants of $I(t)$ obey $C_n < \infty$ for all n, then for either stochastic K or deterministic K_0, the moment generating function $Q_I(s)$ may be expressed in terms of the cumulants of the random variable I. By definition,

[1] Equation (6) in [10] contains typographical errors. Equation (19) in this paper provides the correct result.

$$\ln Q_I(s) = \sum_{n=1}^{\infty} \frac{(-1)^n C_n s^n}{n!} \quad (25)$$

so that

$$Q_I(s) = \exp\left[\sum_{n=1}^{\infty} \frac{(-1)^n C_n s^n}{n!}\right]. \quad (26)$$

For the particular case $\beta \neq 1/n$ for all integers n, we obtain

$$Q_I(s) = \exp\left[\mu \sum_{n=1}^{\infty} \frac{(-1)^n}{n!} \langle K^n \rangle \frac{A^{1-n\beta} - B^{1-n\beta}}{n\beta - 1} s^n\right]. \quad (27)$$

Equations (17) and (19) admit $A = 0$, $B = \infty$, and arbitrary β, whereas (26) does not allow $B = \infty$ for $\beta \leq 1$, nor $A = 0$ for any β. In addition, (27) is not valid for $\beta = 1/n$. However, (26) and (27) are valid for stochastic K as well as deterministic K_0.

V. Amplitude Probability Density Functions

A. *Lévy-Stable Forms ($\beta > 1$)*

Values of the amplitude probability density function $P(I)$ may be obtained from the moment generating function by several methods. If $A = 0$ and $B = \infty$, for $\beta > 1$, and for either deterministic or stochastic K, the amplitude probability density function is Lévy stable with dimension $D \equiv 1/\beta$. $P(I)$ may be calculated either by the Fourier integral [8], [14], [18]

$$P(I) = \frac{1}{\pi} \operatorname{Re} \int_0^{\infty} \exp\left[-j\omega I - \mu \langle K^D \rangle \cdot \Gamma(1-D)(-j\omega)^D\right] d\omega, \quad (28)$$

or the infinite sum [8], [21], [22]

$$P(I) = \frac{1}{\pi I} \sum_{n=1}^{\infty} \frac{(-1)^{n+1} \Gamma(1+nD) \sin(\pi n D)}{n!} \cdot \left[\frac{\mu \Gamma(1-D) \langle K^D \rangle}{I^D}\right]^n. \quad (29)$$

For large values of I the sum converges quickly; for small values of I the integral is more readily implemented by numerical integration techniques [23].

For the particular case $D = 1/2$ the amplitude probability density function assumes the well-known closed form [8], [13], [14]

$$P(I) = \frac{\mu \langle K^{1/2} \rangle}{2} I^{-3/2} \exp\left(-\frac{\mu^2 \pi \langle K^{1/2} \rangle^2}{4I}\right). \quad (30)$$

Fig. 4 displays Lévy-stable amplitude probability density functions for three values of the dimension D.

Furthermore, if $A = 0$ and $\beta > 1$, but $B < \infty$, then the amplitude probability density function will approach a Lévy-stable form as $\mu \to \infty$. This is readily understood since the resulting impulse response function is the same as in the $B = \infty$ case except for the missing tail. Since the missing area is finite, and the total area is infinite, the difference is negligible for large μ (see Appendix B). The limiting distribution will therefore be a Lévy-stable random variable with extreme asymmetry, associated dimension $D \equiv 1/\beta$, and scaling factor $[\mu\Gamma(1-D)]^{1/D} K_0$, as for $B = \infty$ as shown in Section IV-B. Finally, if $A > 0$ and $\beta > 1$, $P(I)$ converges to the Gaussian density for arbitrary B since the area under the impulse response function and under its square are both finite.

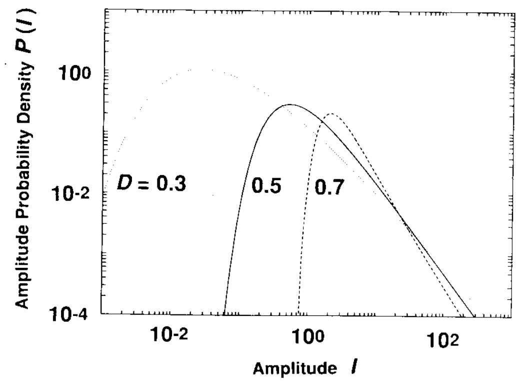

Fig. 4. Double logarithmic plot of Lévy-stable amplitude probability density $P(I)$ vs. I given in (28)–(30) for three values of fractal dimension D: 0.3, 0.5, and 0.7 ($A = 0$, $B = \infty$, $K_0 = 1$, $\mu = 1$). Note long power-law tails for all values of D.

The Lévy-stable shot-noise process developed here is fundamentally different from fractional Brownian motion (FBM), developed by Mandelbrot and Van Ness [15], [16]. FBM has an amplitude distribution determined by the increments in its definition, and may have any amplitude distribution, although FBM is usually Gaussian. For Gaussian FBM the *times between level crossings* exhibit a Lévy-stable time distribution with dimension between 0 and 1. Our Lévy-stable shot-noise process, however, has a Lévy-stable *amplitude* distribution. The Lévy-stable quality derives from the shape of the impulse response functions and the nature of the shot-noise process itself, and is not dependent on a Lévy-stable process in its definition. The level crossings for our Lévy-stable shot-noise process are nonexistent for levels ≤ 0, whereas for sufficiently high levels they approach the driving Poisson process, yielding exponential times between crossings. The distribution of times between the level crossings of our Lévy-stable shot-noise process is never Lévy-stable; only the amplitude of the process is.

Furthermore, the fractal nature of our Lévy-stable shot-noise process differs from that of FBM, which is self-affine and nonstationary. Scaling both the time and amplitude axes of a FBM process by related amounts yields a new FBM process that is statistically identical to the original one, so that $c^{-D} B_D(ct) \sim B_D(t)$, where $B_D(\cdot)$ is a FBM with dimension D, and c is some constant [15]. However, our Lévy-stable process has identical first-order statistics for all time, so $I(ct) \sim I(t)$. Thus FBM is nonstationary, having moments that increase with time, while our Lévy-stable process is strict-sense stationary for all finite times t.

B. Power-Law Tails

All of the Lévy-stable probability densities have long power-law tails (see Fig. 4). Indeed, for $A=0$, $B=\infty$, $\beta>1$, and $D\equiv 1/\beta$, $P(I)$ approaches a simple asymptotic form in the limit $I\to\infty$. Examining (29) it is clear that all terms are of the form $a_n I^{-(1+nD)}$, so that for $I\to\infty$ the $n=1$ term dominates

$$P(I)\to\frac{1}{\pi I}\frac{(-1)^2\Gamma(1+D)\sin(\pi D)}{1!}\left[\frac{\mu\Gamma(1-D)\langle K^D\rangle}{I^D}\right]$$
$$=\frac{\mu\Gamma(1+D)\Gamma(1-D)\sin(\pi D)\langle K^D\rangle}{\pi}I^{-(1+D)}. \quad (31)$$

Using well-known properties of the gamma function [24], we obtain

$$P(I)\approx\mu D\langle K^D\rangle I^{-(1+D)},\qquad I\to\infty. \quad (32)$$

This is indeed expected, since the tail of a Lévy-stable density function of dimension D is known to be power-law with exponent $-(1+D)$.

C. General Expressions

In all cases with deterministic $h(t)$, that is, for any $\beta>0$, the amplitude probability density function of power-law shot noise may be found by evaluating the Fourier integral [8], [18]

$$P(I)=\frac{1}{\pi}\operatorname{Re}\int_0^\infty \exp\left[-j\omega I-\mu\int_A^B\left(1-e^{j\omega K_0 t^{-\beta}}\right)dt\right]d\omega, \quad (33)$$

which is, unfortunately, often difficult. However, the amplitude probability density function may alternatively be obtained for positive I from an integral equation [17] (see Appendix C). We note that if $B<\infty$, then $\Pr\{I=0\}=e^{-\mu(B-A)}>0$, so the density will have a delta function at $I=0$. The amplitude probability density function is given by

$$P(I)=\begin{cases}0, & I<0;\\ e^{-\mu(B-A)}\delta(I), & I=0;\\ 0, & 0<I\le K_0B^{-\beta};\\ \dfrac{\mu K_0^{1/\beta}}{\beta I}\displaystyle\int_{K_0B^{-\beta}}^{I}P(I-u)u^{-1/\beta}\,du, & K_0B^{-\beta}<I<K_0A^{-\beta};\\ \dfrac{\mu K_0^{1/\beta}}{\beta I}\displaystyle\int_{K_0B^{-\beta}}^{K_0A^{-\beta}}P(I-u)u^{-1/\beta}\,du, & I\ge K_0A^{-\beta}.\end{cases} \quad (34)$$

If $B=\infty$, (34) simplifies to

$$P(I)=\frac{\mu K_0^{1/\beta}}{\beta I}\int_0^{\min(I,K_0A^{-\beta})}P(I-u)u^{-1/\beta}\,du, \quad (35)$$

and the integral-equation solution must be multiplied by a scaling constant, determined by requiring $\int_0^\infty P(I)\,dI=1$. The results obtained from the integral equation for $\beta>1$ are then identical to those given for the Lévy-stable case

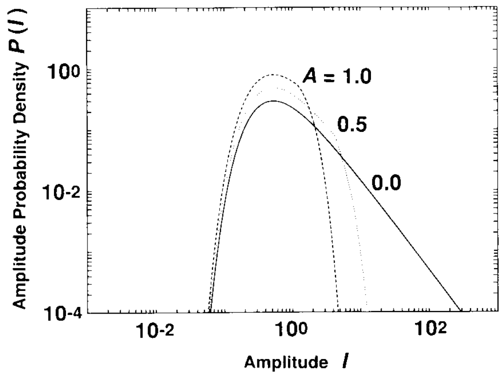

Fig. 5. Double logarithmic plot of amplitude probability density $P(I)$ vs. I in (35) for three values of parameter A shown in Fig. 2: $A=1.0$, 0.5, and 0.0 (Lévy stable) [$\beta=2$ ($D=1/2$), $B=\infty$, $K_0=1$, $\mu=1$]. Solid curve is same as solid curve in Fig. 4. For small values of I amplitude probability density functions differ only by scaling parameter.

for small values of I, except for a scaling constant to normalize the amplitude probability density function to unit area. In that case, the values for the Lévy-stable amplitude probability density function, which are more easily calculated, may be used for values of I between zero and $K_0A^{-\beta}$. Fig. 5 shows the amplitude probability density functions approaching a Lévy-stable form as the starting time A decreases towards zero.

D. Convergence to Gaussian Form

If $C_n<\infty$ for all n, then the amplitude probability density function $P(I)$ satisfies the conditions of the central limit theorem, and therefore approaches a Gaussian density [$N(\cdot)$] as $\mu\to\infty$. This is always the case for $A>0$ and $B<\infty$ [see (12)], as shown in the right-most column of Fig. 3. The mean and variance of the resulting amplitude density will be given by the first and second cumulants, respectively [see (13)], so the limiting form will be

$$P(I)\to N(I\colon C_1,C_2)=(2\pi C_2)^{-1/2}\exp\left[-\frac{(I-C_1)^2}{2C_2}\right]. \quad (36)$$

For finite μ, and for values of I close to the mean of the process (C_1), the amplitude probability density function may be expanded as an infinite sum of polynomials in I multiplied by the limiting amplitude density [18]

$$P(I)\approx N(I\colon C_1,C_2)-\frac{C_3}{6}N^{(3)}(I\colon C_1,C_2)+\left[\frac{C_4}{24}N^{(4)}(I\colon C_1,C_2)-\frac{C_3^2}{72}N^{(6)}(I\colon C_1,C_2)\right]+\cdots, \quad (37)$$

where

$$N^{(0)}(I\colon C_1,C_2)\equiv N(I\colon C_1,C_2), \quad (38)$$

and

$$N^{(n)}(I\colon C_1,C_2)\equiv\frac{\partial^n}{\partial I^n}N(I\colon C_1,C_2),\qquad n>0. \quad (39)$$

The first term on the right-hand side of (37) varies as $\mu^{-1/2}$, the second as μ^{-1}, the third (in square brackets) as $\mu^{-3/2}$, and subsequent terms as higher powers of $\mu^{-1/2}$. For I near C_1, and μ large, the second term in (37) (first-correction term) represents the convergence of the density function to Gaussian form

$$P(I) \approx N(I: C_1, C_2) - \frac{C_3}{6} N^{(3)}(I: C_1, C_2)$$
$$= N(I: C_1, C_2)\left\{1 - \frac{C_3}{6C_2^{3/2}}\left[3\left(\frac{I-C_1}{\sqrt{C_2}}\right) - \left(\frac{I-C_1}{\sqrt{C_2}}\right)^3\right]\right\}$$
$$= N(I: C_1, C_2)\left[1 - \frac{C_3}{2C_2^2}(I - C_1) + \frac{C_3}{6C_2^3}(I - C_1)^3\right]. \quad (40)$$

Fig. 6 illustrates the approach of the amplitude probability density functions to Gaussian form as the driving rate μ increases. To make comparison easier, the amplitude probability density is given in terms of the standardized amplitude z, defined by $z \equiv (I - E[I])/(\text{var}\, I)^{1/2} = (I - C_1)/C_2^{1/2}$. Note that z has zero mean and unity variance by construction.

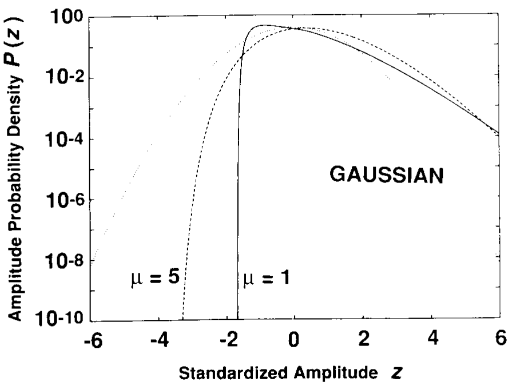

Fig. 6. Semilogarithmic plot of amplitude probability density $P(z)$ vs. z in (35) for two values of driving rate μ: $\mu = 1$ and 5 ($\beta = 2$, $A = 1$, $B = \infty$, $K_0 = 1$). Nonzero value of A causes $P(z)$ to approach Gaussian form, which is shown for comparison. Probability density is given in terms of standardized amplitude variable z, obtained from amplitude I by subtracting mean and dividing by standard deviation.

VI. Autocorrelation Functions

The autocorrelation function is given by

$$R_I(\tau) \equiv E[I(t)I(t+\tau)] = E[I]^2 + \mu R_h(\tau) \quad (41)$$

where the autocorrelation function of $h(K,t)$ itself is

$$R_h(\tau) \equiv \left\langle \int_{-\infty}^{\infty} h(K,t)h(K,t+|\tau|)\, dt \right\rangle$$
$$= \int_A^{B-|\tau|} \langle K^2 \rangle t^{-\beta}(t+|\tau|)^{-\beta}\, dt$$
$$= \langle K^2 \rangle \int_A^{B-|\tau|} (t^2 + |\tau| t)^{-\beta}\, dt. \quad (42)$$

Note that when $|\tau| \geq B - A$, $R_h(\tau) = 0$ so that $R_I(\tau) = E[I]^2$. Under the following conditions the integral in (42) is infinite and therefore $R_I(\tau)$ does not exist:

$$\beta \leq \tfrac{1}{2} \text{ and } B = \infty;$$
$$\beta \geq 1 \text{ and } A = 0;$$
$$\beta \geq \tfrac{1}{2},\ A = 0, \text{ and } \tau = 0. \quad (43)$$

Furthermore, this integral is not solvable analytically except for the case where 2β is a positive integer.

We solve for $R_h(\tau)$ in the three cases $\beta = 1/2$ ($B < \infty$, and $\tau \neq 0$ for $A = 0$), $\beta = 1$ ($A \neq 0$), and $\beta = 2$ ($A \neq 0$) (see Appendix D).

For $\beta = 1/2$

$$R_I(\tau) = \begin{cases} E[I]^2 + 2\mu\langle K^2 \rangle \ln\left[\dfrac{B^{1/2} + (B - |\tau|)^{1/2}}{A^{1/2} + (A + |\tau|)^{1/2}}\right], & 0 \leq |\tau| < B - A; \\ E[I]^2, & |\tau| \geq B - A. \end{cases} \quad (44)$$

For $\beta = 1$

$$R_I(\tau) = \begin{cases} E[I]^2 + \mu\langle K^2 \rangle [A^{-1} - B^{-1}], & \tau = 0; \\ E[I]^2 + \mu \dfrac{\langle K^2 \rangle}{|\tau|} \ln[(1 - |\tau|/B)(1 + |\tau|/A)], & 0 < |\tau| < B - A; \\ E[I]^2, & |\tau| \geq B - A. \end{cases} \quad (45)$$

For $\beta = 2$

$$R_I(\tau) = \begin{cases} E[I]^2 + \dfrac{\mu\langle K^2 \rangle}{3}[A^{-3} - B^{-3}], & \tau = 0; \\ E[I]^2 + \mu\langle K^2 \rangle \left\{ \dfrac{2A + |\tau|}{|\tau|^2 A(A + |\tau|)} - \dfrac{2B - |\tau|}{|\tau|^2 B(B - |\tau|)} + \dfrac{2}{|\tau|^3} \ln[(1 - |\tau|/B)(1 + |\tau|/A)] \right\}, & 0 < |\tau| < B - A; \\ E[I]^2, & |\tau| \geq B - A. \end{cases}$$
(46)

For $A > 0$, $B = \infty$, and $\beta > 1$, it is shown in Appendix D that the autocorrelation function $R_I(\tau)$ approaches a simpler form in the limit $|\tau| \to \infty$

$$R_I(\tau) \to E[I]^2 + \mu\langle K^2\rangle \frac{A^{1-\beta}}{\beta - 1}|\tau|^{-\beta}$$
$$= E[I]^2 + E[I]\frac{\langle K^2\rangle}{\langle K\rangle}|\tau|^{-\beta}, \qquad |\tau| \to \infty, \quad (47)$$

illustrating that it exhibits power-law behavior with the same power-law exponent as the impulse response function. Fig. 7 displays the autocorrelation functions $R_I(\tau)$ for power-law shot-noise with the three values of the power-law exponent β calculated previously: 1/2, 1, and 2. The curves assume an approximately power-law form with exponent $-\beta$ for much of their range, and decrease to $E[I]^2$ for $\tau \geq B - A$.

VII. Power Spectral Densities

All properties of a shot-noise process are determined by the rate μ of the driving Poisson point process and the impulse response function $h(t)$ of the associated linear filter. In particular, Carson's theorem [18] gives the power spectral density $S_I(f)$ [4], [19] of the power-law shot-noise process I in terms of μ and the Fourier transform $\mathscr{F}$ of a normalized version of the impulse response function in (4). We denote this transform by $H(f)$, and obtain

$$H(f) \equiv \mathscr{F}\{h(t)/K\} = \int_A^B t^{-\beta}e^{-j2\pi ft}\,dt$$
$$= [\Gamma(1-\beta, j2\pi fA) - \Gamma(1-\beta, j2\pi fB)](j2\pi f)^{\beta-1}. \quad (48)$$

When the autocorrelation function has a finite integral (see Appendix E), Carson's theorem may be applied,

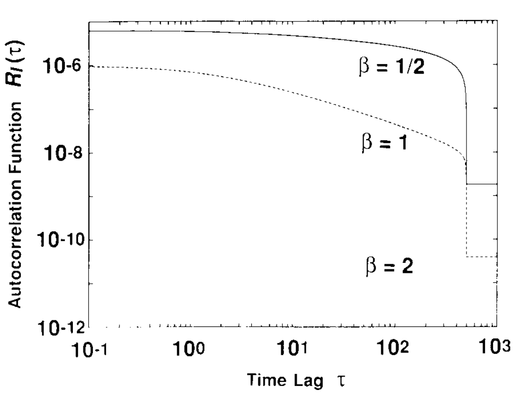

Fig. 7. Double logarithmic plot of autocorrelation functions $R_I(\tau)$ vs. τ given in (44)–(46) for three values of power-law exponent β: 1/2, 1, and 2 ($A = 1$, $B = 501$, $K_0 = 1$, $\mu = 10^{-6}$). Autocorrelation functions exhibit approximate power-law behavior with exponent β for good portion of their range. Note decrease of $R_I(\tau)$ near $\tau = B - A = 500$.

yielding

$$S_I(f) = E[I]^2\delta(f) + \mu\langle K^2\rangle |H(f)|^2$$
$$= E[I]^2\delta(f) + \mu\langle K^2\rangle |\Gamma(1-\beta, j2\pi fA) - \Gamma(1-\beta, j2\pi fB)|^2 (2\pi f)^{2\beta-2}. \quad (49)$$

For the case $0 < \beta < 1$, it is useful to define $\alpha \equiv 2(1-\beta)$. If $A = 0$ and B is finite, then (49) reduces to

$$S_I(f) = E[I]^2\delta(f) + \mu\langle K^2\rangle \cdot |\Gamma(\alpha/2) - \Gamma(\alpha/2, j2\pi fB)|^2 (2\pi f)^{-\alpha}. \quad (50)$$

From (48), the power spectral density[2] can be seen to approach a constant value in the limit $f \to 0$

$$\lim_{f\to 0} S_I(f) = \mu\langle K^2\rangle \frac{B^\alpha}{(\alpha/2)^2}, \quad (51)$$

whereas in the limit $f \to \infty$, the incomplete gamma function in (50) approaches zero, so

$$S_I(f) \to \mu\langle K^2\rangle \Gamma^2(\alpha/2)(2\pi f)^{-\alpha}, \qquad f \to \infty. \quad (52)$$

If B were increased, we would obtain the same behavior for high frequencies, but different and nontrivial behavior for low frequencies. In the limit $B \to \infty$, with $A = 0$ and $0 < \alpha < 2$, mechanical calculation of the power spectral density provides

$$S_I(f) = E[I]^2\delta(f) + \mu\langle K^2\rangle \Gamma^2(\alpha/2)(2\pi f)^{-\alpha}, \quad (53)$$

indicating $1/f^\alpha$ behavior for all frequencies. In this limit, however, the process never reaches a steady state, as shown in Section IV-C. In power-law shot noise, as in other processes, stationarity and $1/f$ behavior over all frequencies are mutually exclusive. Indeed, for $\beta \leq 1$ and $B = \infty$, the process is degenerate, being infinite with probability one as shown in Appendix A, so the concept of power spectral density has limited applicability. Because the impulse response functions have Fourier transforms, a power spectral density can be constructed by the blind application of Carson's theorem. However, this is *not* the Fourier transform of an autocorrelation function since the autocorrelation function and all the moments, including the mean, are infinite.

As summarized in Fig. 3, novel $1/f$-type behavior of the power spectral density is observed in the regime $0 < \beta < 1$. In contrast, novel (Lévy-stable) behavior of the amplitude probability density function is observed only in the regime $\beta > 1$.

VIII. Applications

Power-law shot noise has widespread applicability in engineering and physics since both Poisson events and power-law behavior are ubiquitous. We consider several applications: $1/f$ shot noise, Cherenkov radiation for a random stream of charged particles, diffusion of randomly injected concentration packets, quantum-wire elec-

[2] Equation (5) in [9] contains a typographical error. Equation (51) in this paper provides the correct result.

tric fields, and the mass distribution of solid-particle aggregates.

A. $1/f$ Shot Noise

Noise which has a power spectral density inversely proportional to frequency is called $1/f$ noise [12], [25]–[28]. This noise appears in many diverse environments, including resistors and semiconductors [29]–[31], vacuum tubes [32], and mechanical [33], chemical [34], biological [35], and optical (photon-counting) systems [36]. One widely used theoretical approach to this problem makes use of a superposition of relaxation processes of different time constants [28], [37], [38]. An alternative approach recognizes that integration in the time domain corresponds to a factor of $1/f^2$ in the frequency domain, and offers fractional integration of white noise as a source of $1/f$ noise [39]. Still another approach, suggested by Schönfeld [11] and considered further by van der Zeil [12], concerns shot noise with an impulse response function that decays as $t^{-1/2}$.

More generally, power-law shot noise provides a useful model for $1/f^\alpha$ noise, when $0<\alpha<2$ $(0<\beta<1)$. As shown in Section VII, when $A \to 0$ and $B \to \infty$ the power spectral density varies over all frequencies as $f^{-\alpha}$; it is precisely $1/f$ for $\alpha=1$ $(\beta=1/2)$ [11].

In this limit however, the power spectral density has infinite energy. This poses a problem that can be solved in one of three ways. First, the outer cutoff of the impulse response function B may be decreased from infinity to a finite value [12], in which case (50) provides

$$S_I(f)=E[I]^2\delta(f)+\mu\langle K^2\rangle \cdot\left|\Gamma(\alpha/2)-\Gamma(\alpha/2,j2\pi fB)\right|^2(2\pi f)^{-\alpha}. \quad (54)$$

For low frequencies f, the second gamma function will approximately cancel with the first, thereby reducing the energy to a finite value. For high frequencies, the second gamma function will vanish, yielding the same result as for $B \to \infty$. The second method is to make the area of the impulse response function finite by multiplying it by an exponentially decaying function [25], [26]

$$h^*(K,t)\equiv Kt^{-\beta}e^{-\omega_0 t}, \quad (55)$$

which yields

$$S_I^*(f)=E[I]^2\delta(f) +\mu\langle K^2\rangle\Gamma^2(\alpha/2)\left[\omega_0^2+(2\pi f)^2\right]^{-\alpha/2}. \quad (56)$$

Again the power spectral density has finite energy in the neighborhood of $f=0$ and behaves as $1/f^\alpha$ for high frequencies. Finally the physical limitations of any real experiment used to measure the power spectral density may be imposed on the system. Since the experiment must be conducted in finite time, those components of the power spectral density with frequencies lower than the reciprocal of the duration of the experiment will be excluded. Similarly, since any measuring apparatus has a finite frequency response, those components of the power spectral density at high frequencies will also be excluded. Since the power spectral density is effectively truncated at both low and high frequency limits, the total energy will be finite for any value of α in the range $0<\alpha<2$ and any possible experimental measurement [12], [25].

Fig. 8 shows the shot-noise power spectral densities obtained with $\alpha=1$ $(\beta=1/2)$ for two types of power-law impulse response functions as given in (4): no cutoff ($A=0$ and $B=\infty$), and abrupt cutoff ($A=0$ and $B=1000$). Also shown is the exponential decay result obtained by using (55) and (56) with $\omega_0=\pi/4000$. The power spectral densities all take the form $1/f^\alpha$ with $\alpha=1$ for high frequencies. Note that the abrupt cutoff in the time domain gives rise to oscillations in the frequency domain.

B. Cherenkov Radiation from a Random Stream of Charged Particles

Charged particles traveling faster than the group velocity of light c/n in a transparent medium will radiate electromagnetic fields, often in the visible range. This phenomenon was first examined systematically in a series of experiments by Cherenkov beginning in 1934. In this section we use classical electromagnetic theory to show that the fields produced by Cherenkov radiation arising from a random stream of charged particles may be modeled by the power-law shot-noise process.

Consider a charged particle traveling along the positive x-axis through a transparent, nonferromagnetic medium of refractive index n, at a speed $v>c/n$ (see Fig. 9). We define $J\equiv[(nv/c)^2-1]^{1/2}$, a measure of the amount by which the particle velocity exceeds the Cherenkov limit $v=c/n$, and of the total energy production per unit time. The electric and magnetic fields are calculated at a distance d from the x-axis, where the arbitrary point in the

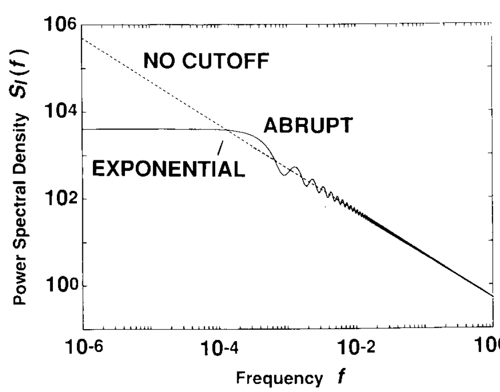

Fig. 8. Power spectral densities for $1/f$ shot noise with different cutoffs: $A=0$ and $B=\infty$ (no cutoff); $A=0$ and $B=1000$ (abrupt cutoff); and exponential cutoff with $\omega_0=\pi/4000$. Note that power spectral densities exhibit $1/f^\alpha$ behavior with exponent $\alpha=1$ for high frequencies, and that abrupt cutoff in impulse response function gives rise to oscillations in frequency domain.

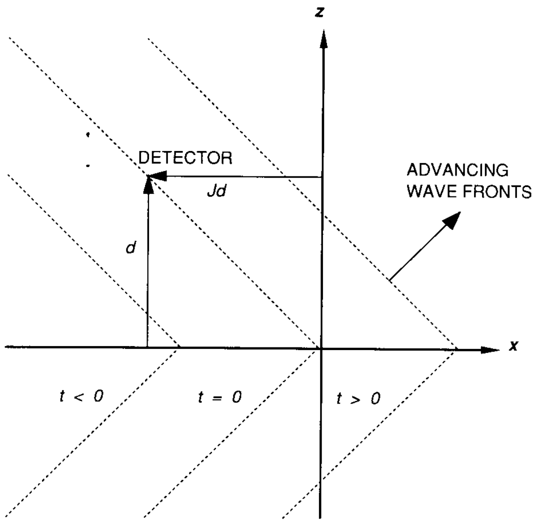

Fig. 9. Charged particle moving faster than speed of light in medium emits Cherenkov radiation. Detector placed at $\{-Jd, 0, d\}$ will measure electric and magnetic fields that decay as inverse power-law functions of time. Wavefronts are shown for particle traveling along X-axis at $t<0$, $t=0$, and $t>0$.

x-z plane $\{-Jd, 0, d\}$ is chosen for algebraic simplicity. We assume that the particle does not experience substantial deceleration while it is significantly close to this point. Following Jelley [40] and Zrelov [41], we obtain scalar and vector potentials satisfying the Lorenz gauge condition

$$\phi = 2qn^{-2}\left[(x-vt)^2 - J^2(y^2+z^2)\right]^{-1/2}, \quad (57)$$

$$A = \frac{n^2}{c} v\phi, \quad (58)$$

respectively, where q is the charge of the particle.

The corresponding fields are

$$\begin{aligned} E &= -\nabla\phi - \frac{1}{c}\frac{\partial A}{\partial t} \\ &= -\frac{2qJ^2}{n^2}\left[(x-vt)^2 - J^2(y^2+z^2)\right]^{-3/2}\{x-vt, y, z\} \\ &= \frac{2qJ^2}{n^2}\left[(vt)^2 + 2Jdvt\right]^{-3/2}\{(vt+Jd), 0, -d\} \\ &= \frac{2qJ^2}{n^2v^2}\left[t^2 + 2t_1 t\right]^{-3/2}\{t+t_1, 0, -d/v\}, \end{aligned} \quad (59)$$

where $t_1 \equiv Jd/v = d(n^2c^{-2} - v^{-2})^{1/2}$. Since the medium is nonferromagnetic,

$$\begin{aligned} H &= B \\ &= \nabla \times A \\ &= \frac{2qv}{c}\left[(x-vt)^2 - J^2(y^2+z^2)\right]^{-3/2}\{0, J^2z, -J^2y\} \\ &= \frac{2qdvJ^2}{c}\left[(vt)^2 + 2Jdvt\right]^{-3/2}\{0,1,0\} \\ &= \frac{2qdJ^2}{cv^2}\left[t^2 + 2t_1 t\right]^{-3/2}\{0,1,0\}. \end{aligned} \quad (60)$$

The foregoing is valid for times when the quantity in the square brackets in (59) and (60) is positive, namely for $t>0$; for $t<0$, the shock wave generated by the particle has not yet reached the detector and all fields are zero. All components of the electric and magnetic fields show power-law decay with a power-law exponent that increases at the crossover time $t = t_1$. No real system will pass frequency components of arbitrarily high frequency, and indeed all systems have practical limits to the frequency components that may be observed at the output. The difference between the upper and lower frequency limits is called the system bandwidth, $\Delta\nu$. Similarly, the onset time of the light pulse will be limited to a value roughly equal to the inverse of the bandwidth; we define $t_0 = 1/\Delta\nu$. In addition, the nonzero size of the charged particle imposes a limit on the onset time [41], although this limit will be relatively unimportant since we assume that the particle is smaller than the wavelength of the generated electromagnetic radiation.

For times larger than the onset time t_0 but still less than t_1, the fields will decay approximately as a simple power law with exponent 3/2:

$$E_x \propto t^{-3/2} \qquad E_z \propto t^{-3/2} \qquad H_y \propto t^{-3/2}. \quad (61)$$

For $t > t_1$, the fields decay more rapidly

$$E_x \propto t^{-2} \qquad E_z \propto t^{-3} \qquad H_y \propto t^{-3}. \quad (62)$$

Even for relatively narrow bandwidths, the onset time t_0 will often be several orders of magnitude smaller than t_1, ensuring a large range of times for which $t^{-3/2}$ behavior is observed. In the wavelength range 536–556 nm as studied by Cherenkov in 1938, for example, the onset time is calculated to be $t_0 \approx 50$ fs. Particles traveling close to the speed of light through materials with a refractive index as low as 1.2, with d as small as 1 cm to the detector yield a crossover time $t_1 \approx 22$ ps. For such particles we can make the approximation that $h(t)=0$ for $t<t_0$, and similarly $h(t)=0$ for $t>t_1$, since the power-law decay exponent increases at $t=t_1$. The electric and magnetic field time response functions due to a single charged particle emitting Cherenkov radiation may then be closely approximated by

$$h(t) = \begin{cases} K_0 t^{-3/2}, & A<t<B; \\ 0, & \text{otherwise}, \end{cases} \quad (63)$$

where we identify $A = t_0$ and $B = t_1$.

In media whose index of refraction differs only slightly from unity, the power-law crossover time t_1 of the impulse response function $h(t)$ will be very small, often smaller than the onset time t_0. In that case the field time response functions will lack the $t^{-3/2}$ portions. However, since the field strength is proportional to J^2, if the index of refraction differs only slightly from unity, then J will be small, and the field strength will be small.

Thus a single particle gives rise to electric and magnetic fields whose strength follows a decaying power-law time function. If a number of particles travel along the x-axis, they will stimulate independent fields. Radioactive sources, such as alpha- and beta-emitters, and particle accelerators operated at low current levels generate Poisson time sequences of energetic charged particles with essentially identical positions and velocities. When these particles pass through a transparent medium under the conditions previously specified, the superposition fields emanating from the medium will obey the power-law shot-noise process.

C. Diffusion of Randomly Injected Concentration Packets

Diffusion provides a broad area of applicability for the power-law shot-noise model. In classical diffusion, particle concentrations decrease in a power-law fashion. Consider a concentration of infinitesimal particles U_0, all initially at some point $\boldsymbol{x} = \boldsymbol{x}_0$ of a d-dimensional space ($d < 4$), at starting time $t = 0$. Then the concentration at $\boldsymbol{x} = \boldsymbol{0}$ at some later time t will be represented by a Gaussian density with a variance that increases with time in a power-law fashion [42]

$$\begin{aligned} U(t) &= U_0(4\pi\Delta t)^{-d/2} \exp\left(-\frac{|\boldsymbol{x}_0|^2}{4\Delta t}\right) \\ &= K_0 e^{-t_0/t} t^{-d/2}, \end{aligned} \tag{64}$$

where $K_0 \equiv U_0(4\pi\Delta)^{-d/2}$, $t_0 \equiv |\boldsymbol{x}_0|^2/4\Delta$, and Δ is the diffusion constant. Except for a rapidly decaying transient near $t = 0$, negligible when $t > 5t_0$, the concentration $U(t)$ varies as $t^{-d/2}$, and thus decays as a power-law function. If we assume that the particles have some lifetime t_1, resulting in $U(t) \approx 0$ for $t > t_1$, the local concentration of the particles may be described in terms of our impulse response function

$$h(t) = \begin{cases} K_0 t^{-d/2}, & A < t < B, \\ 0, & \text{otherwise}, \end{cases} \tag{65}$$

where we identify $A = t_0$ and $B = t_1$.

Finally, if new packets of concentration are deposited at $\boldsymbol{x}_0$ at Poisson times, the overall concentration will be accurately modeled by the power-law shot-noise process. In general, the packets may arrive at points $\boldsymbol{x} \neq \boldsymbol{x}_0$ for some processes, and they need not all have the same initial concentration U_0. The power-law shot-noise model is readily applied to this general case by using the equivalent impulse response function determined by the method of Gilbert and Pollak [17]. Thus diffusion yields a rich area of applicability for power-law shot noise, particularly with exponents $\beta = 1/2$, 1, and $3/2$, corresponding to diffusion in one, two, and three dimensions, respectively. In particular, for the case $\beta = 1/2$, the power spectral density will be precisely $1/f$; thus diffusion in one dimension can give rise to a $1/f$-type spectrum. Other values of β may also be applicable if the particles are constrained to remain on a fractal set, or are of two species that combine in pairs of opposite type.

1) Synaptic Vesicles:

The communication of information between cells in biological systems involves diffusion and provides an important application for power-law shot noise. One cell communicates with another by releasing packets of neurotransmitter (for example, acetylcholine) into the spaces (synaptic clefts) between itself and neighboring cells [43]. Each packet contains many neurotransmitter molecules concentrated into a small volume, which diffuse across the synaptic cleft when released into it. The cells on either side of the cleft are typically close to each other compared to the square root of the active surface areas presented to the cleft, and the cell receiving the neurotransmitter (postsynaptic cell) effectively integrates the concentration of neurotransmitter over its surface as an indication of the strength of the signal. Thus the process may be represented by one-dimensional diffusion. After an effective lifetime t_1, the neurotransmitter molecules are removed by an enzyme (for example, acetylcholinesterase). Thus each packet will result in a concentration over the area of the receiving cell of the form of (65), with $d = 1$. We again identify $A = t_0 = x_0^2/\Delta$ and $B = t_1$, and set K (or K_0) equal to the random (or deterministic) number of neurotransmitter molecules per packet. For a cell under constant stimulation, neurotransmitter packets will often be released into the synaptic cleft in Poisson fashion [43], and the total concentration will therefore be well modeled by power-law shot noise. Finally, we reiterate that since the impulse response functions have a power-law exponent $\beta = 1/2$, the corresponding power spectral density of the process will vary as $1/f^1$. Thus diffusion of neurotransmitter represents a possible source of $1/f$-noise in biological systems.

2) Semiconductor High-Energy Particle Detectors:

Diffusion and power-law shot noise are also important in describing the behavior of semiconductor high-energy particle detectors. A typical detector consists of a lightly doped p-n junction across which a large reverse bias is applied [44]. Energetic charged particles enter the detector, usually along the p-n axis, and create electron-hole pairs within a large part of the semiconductor depletion region. The higher the energy of the particle, the greater the number of electron-hole pairs produced. These carriers are then swept out of the depletion region of the diode by the high reverse-bias field, electrons towards the n region and holes towards the p region. This occurs before many of the electrons and holes recombine. However, some of the carriers do recombine, reducing the detected charge created by the original energetic charged particle, so a description of the recombination process is useful. Consider a single energetic particle entering the detector at a time $t = 0$. We assume that the electron-hole pairs are created instantaneously throughout the semiconductor depletion region, distributed in a three-dimensional Poisson fashion, and that they begin diffusing as soon as they are created. Whenever an electron and a hole approach within some critical radius, the two carriers either annihilate each other immediately or first form an exciton and later recombine. In either case they no longer carry current and may be considered to be annihilated. For now we ignore the drift current; later we will consider the case where drift current is important.

The solution to this semiconductor recombination problem may be adapted from a similar problem that has already been solved: molecular reactions involving two species which combine in pairs [45], [46]. A cursory analysis for a diffusion process would suggest that the concentration of electrons and holes would decay in time as $t^{-d/2}$, and indeed if the distributions of the two types of carriers were highly correlated, then the concentration would follow this form with $d=3$ for three-dimensional diffusion. However, often the carrier distributions are independent, at least over short distances. Consider a sub-volume of the depletion region which, due to the variance of the Poisson distribution, has an excess of electrons at $t=0$. The holes in this section will be annihilated at some later time, but the remaining excess electrons will have to diffuse out of this region before encountering any additional holes, which will require more time, slowing the annihilation process. This effect is seen on all time and length scales, and results in a concentration that decays as $t^{-d/4}$ rather than $t^{-d/2}$. If the particle concentrations are dependent over distances longer than some dependence length l_d, then the concentration will decay as $t^{-d/2}$ for time $t > t_1 = l_d^2/\Delta$ [47], [48]. When electron-hole pairs are created, the electron and hole are initially displaced by a finite length, so the concentrations of electrons and holes will be highly correlated over regions larger than that average length.

Including the effects of drift yields still other exponents. Here the distance traveled by a carrier along the direction of drift increases from $\sim t^{1/2}$ (diffusion alone) to $\sim t^1$ (with drift). Since there are d dimensions, the total volume swept out increases as $\sim t^{d/2}$ with diffusion alone; with drift there are $d-1$ dimensions varying as $\sim t^{1/2}$ each, and one varying as $\sim t^1$, for a total volume increasing as $\sim t^{(d+1)/2}$. Since the particle concentration decays as the inverse square root of the volume encountered, it varies as $t^{-(d+1)/4}$ for independent electron and hole distributions, and as $t^{-(d+1)/2}$ for dependent distributions [49]. In the presence of drift and diffusion, the concentration of particles is therefore given by

$$h(t)=\begin{cases}0, & t<A;\\ Kt^{-(d+1)/4}, & A<t<B;\\ Kt^{-(d+1)/2}, & t>B;\end{cases} \tag{66}$$

where we identify $A = x_0^2/\Delta$ and $B = x_c^2/\Delta$, x_0 being a minimum separation for created electron-hole pairs, x_c being the maximum separation corresponding to a correlation length, and Δ being a combined effective diffusion constant.

If energetic particles impinge on the detector at discrete times corresponding to a one-dimensional Poisson time process, then the resulting electron and hole concentrations will be well described by the power-law shot-noise process. Thus power-law shot noise should prove important in understanding the statistics of carrier recombination within the depletion region of the semiconductor.

3) Diffusion on Fractals:

Finally we turn to diffusion on fractals and percolation structures. In this case, the power-law exponent is given by $\beta = d_s/2$, where d_s is the spectral dimension of the fractal set, defined by

$$d_s \equiv 2d_f/(2+d_d), \tag{67}$$

where d_f is the standard (Hausdorf) fractal dimension, and d_d is the exponent describing the power-law variation of the diffusion constant with distance [50], [51]. For percolation clusters at threshold, the spectral dimension lies between 1 and 2, and approaches a limit of 4/3 for an infinite-dimensional embedding space [51].

D. Quantum-Wire Electric Fields

The magnitude of the electric field at the growing edge of a doped semiconductor whisker or quantum wire is precisely described by the power-law shot-noise process developed here. As growth proceeds, dopant atoms are introduced into the growing edge of the wire in a Poisson fashion. Each ionized donor (or acceptor) atom produces an inverse-square electric field that decays as x^{-2}, where x is the distance from the ionized donor to the edge of the quantum wire. The mobile carriers are uniformly distributed throughout the material so that they do not contribute a spatially varying field. Thus the variation of the electric field at the growing edge of the quantum wire is isomorphic to the power-law shot-noise process with

$$h(t)=\begin{cases}K_0 t^{-\beta}, & A\le t;\\ 0, & \text{otherwise},\end{cases} \tag{68}$$

where A represents some intrinsic cutoff distance associated with the nonzero size of the impurity atoms. Our approach is readily generalized by considering stochastic impulse response functions $h(K,t)$.

Although our general results apply for random *processes*, for some problems it is sufficient to consider the resulting *distributions* associated with this process. At the edge of a quantum wire of fixed length [52], for example, the first-order electric-field statistics arising from the ionized impurity atoms (ignoring the constant field contributed by the free carriers) are given by (34). This is plotted in Fig. 10 for a Te-doped n-type GaAs quantum wire, for which $A = .211$ nm as provided by the ionic radius of tellurium; $B \to \infty$ for a sufficiently long wire; the Coulomb constant $K_0 = q/4\pi\epsilon = 1.32\times10^6$ V/cm-nm^2, where q is the electronic charge and the permittivity ϵ of GaAs is 9.65×10^{-13} F/cm; $\beta=2$; and $\mu = aN_D = 0.004$ nm^{-1} for a wire of cross-sectional area $a = 400$ nm^2 and dopant concentration $N_D = 10^{16}$ cm^{-3}. This density is proportional to, and essentially coincident with, the Lévy-stable density given in (30) for fields as high as

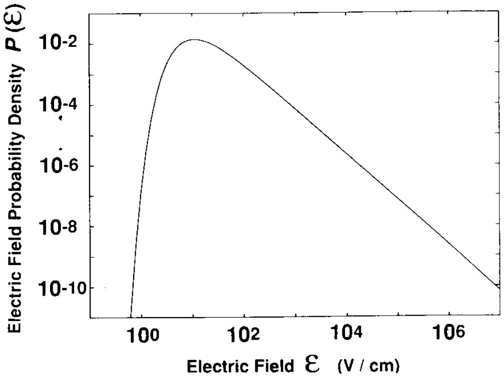

Fig. 10. Double logarithmic plot of electric-field magnitude probability density $P(\mathcal{E})$ vs. $\mathcal{E}$ at edge of a Te-doped GaAs quantum wire with dopant ionic radius $A = 0.211$ nm, area $a = 400$ nm^2, and dopant concentration $N_D = 10^{16}$ cm^{-3}.

2.97×10^7 V/cm. An analogous application is the magnitude of the gravitational field provided by a random distribution of masses [53]. An infinite number of these corresponds to a noncausal power-law form for $h(t)$ and leads to a symmetric Lévy-stable probability density of dimension $D = 1/2$.

E. Mass Distribution of Solid-Particle Aggregates

A useful example of our analysis lies in the domain of solid-particle aggregates, including diffusion-limited aggregates, cluster-cluster aggregates, and aerosols. The mass distribution of the aggregated particles often obeys a power law over some range of masses m in these systems, such that [54]–[56]

$$\Pr\{M \geq m\} = cm^{-D}, \tag{69}$$

where c is a normalizing constant and the power-law exponent D typically falls in the range $0 < D < 1$. The probability distribution for the individual masses is isomorphic to sampling the time function $M(t) = Kt^{-\beta}$ uniformly over some range of times, where again $\beta = 1/D$. The total mass enclosed within a specified region is then isomorphic to the fractal shot-noise amplitude distribution. In particular the enclosed mass has a moment generating function given by (17) and (19), and in the limit by (21).

IX. Conclusion

In this paper we examined the properties of power-law shot noise, which has a number of unique characteristics. We derived some of its statistical properties, including its moments, moment generating functions, amplitude probability density functions, autocorrelation functions, and power spectral densities. Some of these results are summarized in Fig. 3. We showed that for an impulse response function of the form of (4), with $\beta > 1$, $A = 0$, $B = \infty$, and stochastic or deterministic K, the resulting shot-noise amplitude distribution is a Lévy-stable random variable with extreme asymmetry and associated dimension $D \equiv 1/\beta$ for all values μ of the driving Poisson process. If $B < \infty$, then the shot-noise amplitude distribution converges to such a Lévy-stable random variable in the limit $\mu \to \infty$. We also showed that for $0 < \beta < 1$ the resulting power spectral density varies as $f^{-\alpha}$, where the exponent α is defined by $\alpha \equiv 2(1-\beta)$ and varies between 0 and 2. For the particular case $\alpha = 1$, the power spectral density varies precisely as $1/f$, so that power-law shot noise can serve as a form of $1/f$ shot noise. We note that in power-law shot noise the amplitude probability density, autocorrelation function, and power spectral density, as well as the impulse response function itself, all assume power-law behavior, indicating its fractal nature. A number of physical processes that power-law shot noise may describe were considered. Finally, we note that a fractal doubly stochastic Poisson point process (DSPP) can be constructed from power-law shot noise, just as an ordinary DSPP is constructed from ordinary shot noise [7].

Appendix A
Amplitude Probability Distribution for $0 < \beta \leq 1$ and Infinite Tail

For $0 < \beta \leq 1$ and $B = \infty$, the shot-noise process I will be infinite with probability one. To show this, we consider the moment generating function $Q_I(s)$ in (16)

$$Q_I(s) \equiv E[e^{-sI}] = \exp\left[-\frac{\mu(sK_0)^{1/\beta}}{\beta}\int_0^{sK_0A^{-\beta}}\frac{1-e^{-u}}{u^{1+1/\beta}}\,du\right]. \tag{A1}$$

If $s = 0$, then $Q_I(0) = 1$ follows directly from the definition. Otherwise, for $0 < \beta \leq 1$,

$$\int_0^{sK_0A^{-\beta}}\frac{1-e^{-u}}{u^{1+1/\beta}}\,du \geq \int_0^{c}\frac{1-e^{-u}}{u^{1+1/\beta}}\,du \geq \frac{1-e^{-c}}{c}\int_0^{c}\frac{u}{u^{1+1/\beta}}\,du$$
$$= \frac{1-e^{-c}}{c}\int_0^{c}u^{-1/\beta}\,du = +\infty, \tag{A2}$$

where c is any finite real number satisfying $0 < c \leq sK_0A^{-\beta}$. Therefore,

$$Q_I(s) = \exp\left[-\frac{\mu(sK_0)^{1/\beta}}{\beta}\infty\right] = \exp(-\infty) = 0. \tag{A3}$$

Thus $Q_I(s)$ is given by

$$Q_I(s) = \begin{cases}1, & s = 0,\\ 0, & s \neq 0;\end{cases} \tag{A4}$$

so that

$$\Pr\{I < x\} = 0, \qquad \text{for all } x < \infty. \tag{A5}$$

Appendix B
Amplitude Moment Generating Function for $\beta > 1$ and $\mu \to \infty$

For $\beta > 1$, $A = 0$, and $B < \infty$, the amplitude probability density function of the shot-noise process I will approach a Lévy-stable distribution of extreme asymmetry and dimension $D = 1/\beta$ as the rate μ of the driving Poisson process approaches infinity. To show this, we evaluate the form of the moment generating function $Q_I(s)$ given in (19) for $A=0$ using l'Hôpital's rule

$$Q_I(s)=\exp\{-\mu B[1-\exp(-sK_0B^{-1/D})] - \mu(sK_0)^D\Gamma(1-D,sK_0B^{-1/D})\}. \quad \text{(B1)}$$

We now define

$$p\equiv K_0[\mu\Gamma(1-D)]^{1/D}s, \quad \text{(B2)}$$

so that

$$sK_0B^{-1/D}=p[\mu B\Gamma(1-D)]^{-1/D}\equiv pC(\mu), \quad \text{(B3)}$$

where $C(\mu)$ is used to simplify the notation. As $\mu\to\infty$, $C(\mu)\to 0$. The moment generating function becomes

$$Q_I(p)=\exp\left(-\mu B\{1-\exp[-pC(\mu)]\} - p^D\frac{\Gamma[1-D,pC(\mu)]}{\Gamma(1-D)}\right) = \exp\left(-p^D-\mu B\{1-\exp[-pC(\mu)]\} + p^D\frac{\int_0^{pC(\mu)}e^{-t}t^{-D}\,dt}{\Gamma(1-D)}\right). \quad \text{(B4)}$$

It now remains to consider the limiting values of the three terms inside the exponential function shown previously. The first term remains constant at $-p^D$; using l'Hôpital's rule on the second term shows that it approaches zero as μ increases towards infinity; and the third term vanishes as its upper limit approaches zero as μ increases towards infinity. Thus the only term remaining in the limit is the first, and

$$\lim_{\mu\to\infty}Q_I(p)=\exp(-p^D). \quad \text{(B5)}$$

In terms of the original variable, s, the moment generating function is written as

$$Q_I(s)\to\exp[-\mu K_0^D\Gamma(1-D)s^D], \qquad \mu\to\infty. \quad \text{(B6)}$$

Thus, as $\mu\to\infty$, the moment generating function $Q_I(s)$ approaches the Lévy-stable form in (21), and therefore the amplitude probability density function converges in distribution to Lévy-stable form as $\mu\to\infty$.

Appendix C
Integral Equation for the Amplitude Probability Density Function

For finite area impulse response functions and arbitrary β, the amplitude probability density function may be obtained for positive I from an integral equation [17]

$$IP(I)=\mu\int_{-\infty}^{\infty}P[I-h(K_0,t)]h(K_0,t)\,dt = \mu\int P(I-K_0t^{-\beta})K_0t^{-\beta}\,dt. \quad \text{(C1)}$$

Substituting $u\equiv h(K_0,t)=K_0t^{-\beta}$ we obtain (34), which is

$$P(I)=\frac{\mu}{I}\int P(I-u)(u/\beta)K_0^{1/\beta}u^{-1-1/\beta}\,du = \frac{\mu K_0^{1/\beta}}{\beta I}\int P(I-u)u^{-1/\beta}\,du. \quad \text{(C2)}$$

The limits of u in (C2) are found by requiring that $P(I-u)>0$ and that the value of u be attained by the function $h(t)$ for some value of t.

Appendix D
Closed Form Expressions for $R_h(\tau)$

For $\beta=1/2$ and $0\le|\tau|<B-A$,

$$R_h(\tau)=\langle K^2\rangle\int_A^{B-|\tau|}(t^2+|\tau|t)^{-1/2}\,dt = 2\langle K^2\rangle\ln\left[t^{1/2}+(t+|\tau|)^{1/2}\right]_A^{B-|\tau|} = 2\langle K^2\rangle\ln\left[\frac{B^{1/2}+(B-|\tau|)^{1/2}}{A^{1/2}+(A+|\tau|)^{1/2}}\right], \quad \text{(D1)}$$

which is finite if $B<\infty$ and either $A>0$ or $\tau\neq 0$.

For $\beta=1$ and $\tau=0$,

$$R_h(\tau)=\langle K^2\rangle\int_A^B(t^2)^{-1}\,dt=\langle K^2\rangle\int_A^Bt^{-2}\,dt = \langle K^2\rangle[A^{-1}-B^{-1}], \quad \text{(D2)}$$

which is finite if $A>0$.

For $\beta=1$ and $0<|\tau|<B-A$,

$$R_h(\tau)=\langle K^2\rangle\int_A^{B-|\tau|}(t^2+|\tau|t)^{-1}\,dt=\frac{\langle K^2\rangle}{|\tau|}\ln\left[\frac{t}{t+|\tau|}\right]_A^{B-|\tau|} = \frac{\langle K^2\rangle}{|\tau|}\ln[(1-|\tau|/B)(1+|\tau|/A)], \quad \text{(D3)}$$

which is finite if $A>0$.

For $\beta=2$ and $\tau=0$,

$$R_h(\tau)=\langle K^2\rangle\int_A^B(t^2)^{-2}\,dt=\langle K^2\rangle\int_A^Bt^{-4}\,dt = \frac{\langle K^2\rangle}{3}[A^{-3}-B^{-3}], \quad \text{(D4)}$$

which is finite if $A>0$.

For $\beta=2$ and $0<|\tau|<B-A$,

$$R_h(\tau)=\langle K^2\rangle\int_A^{B-|\tau|}(t^2+|\tau|t)^{-2}\,dt = -\langle K^2\rangle\left[\frac{2t+|\tau|}{|\tau|^2t(t+|\tau|)}+\frac{2}{|\tau|^3}\ln\frac{t}{t+\tau}\right]_A^{B-|\tau|} = \langle K^2\rangle\left\{\frac{2A+|\tau|}{|\tau|^2A(A+|\tau|)}-\frac{2B-|\tau|}{|\tau|^2B(B-|\tau|)} + \frac{2}{|\tau|^3}\ln[(1-|\tau|/B)(1+|\tau|/A)]\right\}, \quad \text{(D5)}$$

which is finite if $A>0$. The value at $\tau=0$ may also be determined by taking the limit of the expression for $\tau\neq 0$, and using l'Hôpital's rule twice.

For general $\beta>1$, $A>0$, and $B=\infty$, a simple form for $R_h(\tau)$ can be found in the limit $|\tau|\to\infty$. We first find an upper bound for the integral

$$\int_A^\infty (t^2+|\tau|t)^{-\beta}\,dt = \int_A^\infty t^{-\beta}(t+|\tau|)^{-\beta}\,dt < \int_A^\infty t^{-\beta}(|\tau|)^{-\beta}\,dt = \frac{A^{1-\beta}}{\beta-1}|\tau|^{-\beta}. \quad \text{(D6)}$$

For the lower bound we truncate the integral at some value T

$$\int_A^\infty (t^2+|\tau|t)^{-\beta}\,dt = \int_A^\infty t^{-\beta}(t+|\tau|)^{-\beta}\,dt > \int_A^T t^{-\beta}(T+|\tau|)^{-\beta}\,dt = \frac{A^{1-\beta}-T^{1-\beta}}{\beta-1}(T+|\tau|)^{-\beta}. \quad \text{(D7)}$$

This is valid for any $T > A$. We choose $T = (A|\tau|)^{1/2}$, so that

$$\int_A^\infty (t^2+|\tau|t)^{-\beta}\,dt > \frac{A^{1-\beta}-(A|\tau|)^{(1-\beta)/2}}{\beta-1}\left[(A|\tau|)^{1/2}+|\tau|\right]^{-\beta} = \frac{A^{1-\beta}}{\beta-1}|\tau|^{-\beta}\left[1+(A/|\tau|)^{1/2}\right]^{-\beta}\left[1-(A/|\tau|)^{(\beta-1)/2}\right]. \quad \text{(D8)}$$

Combining limits, we obtain

$$\left[1+(A/|\tau|)^{1/2}\right]^{-\beta}\left[1-(A/|\tau|)^{(\beta-1)/2}\right] < \frac{\int_A^\infty (t^2+|\tau|t)^{-\beta}\,dt}{|\tau|^{-\beta}A^{1-\beta}/(\beta-1)} < 1 \quad \text{(D9)}$$

for all τ: $|\tau| > A$. In the limit $|\tau| \to \infty$, the lower bound approaches 1, so

$$\int_A^\infty (t^2+|\tau|t)^{-\beta}\,dt \to |\tau|^{-\beta}A^{1-\beta}/(\beta-1), \quad \text{(D10)}$$

and

$$R_h(\tau) \to \langle K^2\rangle \frac{A^{1-\beta}}{\beta-1}|\tau|^{-\beta}. \quad \text{(D11)}$$

Appendix E
Power Spectral Density for $0<\beta<1$ and $B<\infty$

For $0<\beta<1$ and $B<\infty$, the autocorrelation function and its Fourier transform exist, and the power spectral density is therefore well defined. To show this we proceed from the definitions. For $f \neq 0$

$$S_I(f) = \int_{\tau=-\infty}^{\infty}\int_{t=-\infty}^{\infty}\langle h(t)h(t+\tau)\rangle e^{-j2\pi f\tau}\,dt\,d\tau = 2\langle K^2\rangle \int_{\tau=0}^{B-A}\int_{t=A}^{B-\tau}(t^2+\tau t)^{-\beta}\cos(2\pi f\tau)\,dt\,d\tau, \quad \text{(E1)}$$

so that

$$\begin{aligned}|S_I(f)| &< 2\langle K^2\rangle \int_{\tau=0}^{B}\int_{t=0}^{B-\tau}(t^2+\tau t)^{-\beta}\,dt\,d\tau \\ &= 2\langle K^2\rangle \int_{t=0}^{B}\int_{\tau=0}^{B-t}(t^2+\tau t)^{-\beta}\,d\tau\,dt \\ &= 2\langle K^2\rangle \int_{t=0}^{B} t^{-\beta}\left(\frac{B^{1-\beta}-t^{1-\beta}}{1-\beta}\right)dt \\ &= \frac{2\langle K^2\rangle}{1-\beta}\left(B^{1-\beta}\int_0^B t^{-\beta}\,dt - \int_0^B t^{1-2\beta}\,dt\right) \\ &= \frac{\langle K^2\rangle B^{2-2\beta}}{(1-\beta)^2} \\ &< \infty. \end{aligned} \quad \text{(E2)}$$

Thus $|S_I(f)| < \infty$ for all frequencies $f \neq 0$, and the power spectral density is therefore well defined for $0<\beta<1$ and $B<\infty$.

References

[1] W. Schottky, "Über spontane Stromschwankungen in verschiedenen Elektrizitätsleitern," *Annalen der Physik*, vol. 57, pp. 541–567, 1918.

[2] N. Campbell, "The study of discontinuous phenomena," *Proc. Cambr. Phil. Soc.*, vol. 15, pp. 117–136, 1909.

[3] N. Campbell, "Discontinuities in light emission," *Proc. Cambr. Phil. Soc.*, vol. 15, pp. 310–328, 1909.

[4] W. B. Davenport, Jr. and W. L. Root, *An Introduction to the Theory of Random Signals and Noise*. New York: McGraw-Hill, 1958.

[5] B. Picinbono, C. Bendjaballah, and J. Pouget, "Photoelectron Shot Noise," *J. Math. Phys.*, vol. 11, pp. 2166–2176, 1970.

[6] A. Papoulis, *Probability, Random Variables, and Stochastic Processes*. New York: McGraw-Hill, 1984.

[7] B. E. A. Saleh and M. C. Teich, "Multiplied-Poisson noise in pulse, particle, and photon detection," *Proc. IEEE*, vol. 70, pp. 229–245, 1982.

[8] W. Feller, *An Introduction to Probability Theory and its Applications*, vol. 2, 3rd ed. New York: Wiley, 1971.

[9] S. B. Lowen and M. C. Teich, "Generalised $1/f$ shot noise," *Electron. Lett.*, vol. 25, pp. 1072–1074, 1989.

[10] S. B. Lowen and M. C. Teich, "Fractal shot noise," *Phys. Rev. Lett.*, vol. 63, pp. 1755–1759, 1989.

[11] H. Schönfeld, "Beitrag zum $1/f$-Gesetz beim Rauschen von Halbleitern," *Z. Naturforsch.*, vol. A10, pp. 291–300, 1955.

[12] A. van der Zeil, "Flicker noise in electronic devices," *Adv. in Elect. and Electron. Phys.*, vol. 49, pp. 225–297, 1979.

[13] P. Lévy, *Calcul des Probabilités*. Paris: Gauthier-Villars, 1925.

[14] P. Lévy, *Théorie de l'Addition des Variables Aléatoires*. Paris: Gauthier-Villars, 1954.

[15] B. B. Mandelbrot and I. W. Van Ness, "Fractional Brownian motions, fractional noises, and applications," *Soc. Ind. and Appl. Math. (SIAM) Rev.*, vol. 10, pp. 422–437, 1968.

[16] B. B. Mandelbrot, *The Fractal Geometry of Nature*. New York: Freeman, 1983.

[17] E. N. Gilbert and H. O. Pollak, "Amplitude distribution of shot noise," *Bell Syst. Tech. J.*, vol. 39, pp. 333–350, 1960.

[18] S. O. Rice, "Mathematical analysis of random noise," *Bell Syst. Tech. J.*, vol. 23, pp. 1–51, 1944; vol. 24, pp. 52–162, 1945 (Reprinted in *Selected Papers on Noise and Stochastic Processes*, N. Wax, Ed. New York: Dover, 1954, pp. 133–294).

[19] J. L. Doob, *Stochastic Processes*. New York: Wilev, 1953.

[20] K. Matsuo, M. C. Teich, and B. E. A. Saleh, "Thomas point process in pulse, particle, and photon detection," *Appl. Optics*, vol. 22, pp. 1898–1909, 1983.

[21] H. Pollard, "The representation of e^{-x^λ} as a Laplace integral," *Bull. Amer. Math. Soc.*, vol. 52, pp. 908–910, 1946.

[22] P. Humbert, "Nouvelles correspondances symboliques," *Bull. Soc. Math. France*, vol. 69, pp. 121–129, 1945.

[23] W. H. Press, B. R. Flannery, S. A. Teukolsky, and W. T. Vetterling, *Numerical Recipes*. Cambridge: Cambridge Univ. Press, 1986.

[24] I. S. Gradshteyn and I. M. Ryzhik, *Table of Integrals, Series and Products*. Orlando, Florida: Academic, 1980, p. 937.

[25] V. Radeka, "$1/f$ noise in physical measurements," *IEEE Trans. Nucl. Sci.*, vol. NS-16, pp. 17–35, 1969.

[26] M. J. Buckingham, *Noise in Electronic Devices and Systems*. New York: Wiley-Halsted, 1983.

[27] A. van der Zeil, "Unified presentation of $1/f$ noise in electronic devices: Fundamental $1/f$ noise sources," *Proc. IEEE*, vol. 76, pp. 233–258, 1988.

[28] M. B. Weissman, "$1/f$ noise and other slow, nonexponential kinetics in condensed matter," *Rev. Mod. Phys.*, vol. 60, pp. 537–571, 1988.

[29] P. H. Handel, "Turbulence theory for the current carriers in solids and a theory of $1/f$ noise," *Phys. Rev. A*, vol. A3, pp. 2066–2073, 1971.

[30] F. N. Hooge, "$1/f$ noise," *Physica*, vol. 83B, pp. 14–23, 1976.

[31] D. A. Bell, "A survey of $1/f$ noise in electrical conductors," *J. Phys. C*, vol. 13, pp. 4425–4437, 1980.

[32] J. B. Johnson, "The Schottky effect in low frequency circuits," *Phys. Rev.*, vol. 26, pp. 71–85, 1925.

[33] T. Geisel, A. Zacherl, and G. Radons, "Generic $1/f$ noise in chaotic Hamiltonian dynamics," Phys. Rev. Lett., vol. 59, pp. 2503–2506, 1987.

[34] T. Musha, K. Sugita, and M. Kaneko, "$1/f$ noise in aqueous $CuSO_4$ solution," in *Noise in Physical Systems and $1/f$ Noise*, M. Savelli, G. Lecoy, and J.-P. Nougier, Eds. New York: Elsevier, 1983, pp. 389–392.

[35] T. Musha, "$1/f$ fluctuations in biological systems," in *Proc. 6th Int. Conf. Noise in Physical Systems*. New York: Elsevier, 1981, pp. 143–146.

[36] T. Musha, "Power spectral density estimation of light intensity fluctuations in photon counting," *Jpn. J. Appl. Phys.*, vol. 26, pp. 2022–2025, 1987.

[37] A. van der Zeil, "On the noise spectra of semi-conductor noise and of flicker effect," *Physica*, vol. 16, pp. 359–372, 1950.

[38] A. L. McWhorter, "$1/f$ noise and related surface effects in germanium," in *Semiconductor Surface Physics*, R. H. Kingston, Ed. Philadelphia: Univ. of Penn., 1956.

[39] J. A. Barnes and D. W. Allan, "A statistical model of flicker noise," *Proc. IEEE*, vol. 54, pp. 176–178, 1966.

[40] J. V. Jelley, *Čerenkov Radiation*. London: Pergamon, 1958.

[41] V. P. Zrelov, *Cherenkov Radiation in High-Energy Physics, Part I.* Atomizdat: Moscow, 1968 (translation—Jerusalem: Israel Program for Scientific Translations, 1970).

[42] M. A. Pinsky, *Introduction to Partial Differential Equations with Applications*. New York: McGraw-Hill, 1984.

[43] S. W. Kuffler, J. G. Nicholls, and A. R. Martin, *From Neuron to Brain*. 2nd ed. Sunderland, MA: Sinauer, 1984.

[44] G. F. Knoll, *Radiation Detection and Measurement*, 2nd ed. New York: Wiley, 1989.

[45] S. F. Burlatsky, G. S. Oshanin, and A. A. Ovchinnikov, "Fluctuation-dominated kinetics of incoherent excitation quenching," *Phys. Lett. A.*, vol. 139, pp. 241–244, 1989.

[46] G. S. Oshanin, S. F. Burlatsky, and A. A. Ovchinnikov, "Fluctuation-dominated kinetics of irreversible bimolecular reactions with external random sources on fractals," *Phys. Lett. A.*, vol. 139, pp. 245–248, 1989.

[47] A. A. Ovchinnikov and Y. B. Zeldovich, "Role of density fluctuations in bimolecular reaction kinetics," *Chem. Phys.*, vol. 28, pp. 215–218, 1978.

[48] D. Toussaint and F. Wilczek, "Particle-antiparticle annihilation in diffusive motion," *J. Chem. Phys.*, vol. 78, pp. 2642–2647, 1983.

[49] K. Kang and S. Redner, "Scaling approach for the kinetics of recombination processes," *Phys. Rev. Lett.*, vol. 52, pp. 955–958, 1984.

[50] S. Alexander and R. Orbach, "Density of states on fractals: 'fractons,'" *J. Phys. Lett.*, vol. 43, pp. L625–L631, 1982.

[51] R. Rammal and G. Toulouse, "Random walks on fractal structures and percolation clusters," *J. Phys. Lett.*, vol. 44, pp. L13–L22, 1983.

[52] P. M. Petroff, A. C. Gossard, R. A. Logan, and W. Wiegmann, "Toward quantum well wires: Fabrication and optical properties," *Appl. Phys. Lett.*, vol. 41, pp. 635–638, 1982.

[53] I. J. Good, "The real stable characteristic functions and chaotic acceleration," *J. Roy. Stat. Soc.*, ser. B, vol. 23, pp. 180–183, 1961.

[54] T. A. Witten, Jr. and L. M. Sander, "Diffusion-limited aggregation, a kinetic phenomenon," *Phys. Rev. Lett.*, vol. 47, pp. 1400–1403, 1981.

[55] P. Grassberger, "On the spreading of two-dimensional percolation," *J. Phys. A*, vol. 18, pp. L215–L219, 1985.

[56] H. Takayasu, I. Nishikawa, and H. Tasaki, "Power-law mass distribution for aggregation systems with injection," *Phys. Rev. A*, vol. 37, pp. 3110–3117, 1988.